

INSTITUTE OF PLASMA PHYSICS

NAGOYA UNIVERSITY

---

# RESEARCH REPORT

NAGOYA, JAPAN

Plasma Confinement in Hybrid Stellarator  
with L=2 and L=3 Helical Fields<sup>†</sup>

K. Miyamoto, M. Fujiwara, K. Kawahata,  
Y. Terashima, T. Dodo\* and K. Yatsu\*\*

IPPJ-199

October 1974

Further communication about this report is to be sent to the Research Information Center, Institute of Plasma Physics, Nagoya University, Nagoya, Japan.

---

† Paper to be presented in the Fifth International Conference on Plasma Physics and Controlled Nuclear Fusion Research.

Permanent address:

\* Central Research Laboratory, Hitachi Limited, Kokubunji, Tokyo.

\*\* Department of Physics, Tokyo University of Education, Tokyo.

## PLASMA CONFINEMENT IN HYBRID STELLARATOR

WITH  $L=2$  AND  $L=3$  HELICAL FIELDS

K. Miyamoto, M. Fujiwara, K. Kawahata,  
Y. Terashima, T. Dodo\* and K. Yatsu\*\*

Institute of Plasma Physics, Nagoya University,  
Nagoya, Japan

Abstract

Dependences of plasma transport on the rotational transform angle and the shear as well as the plasma parameters are studied using JIPP Ib stellarator which equips both  $l=2$  and  $l=3$  helical windings. Afterglow plasmas produced by electron cyclotron resonant heating and P.I.G. discharge are used.

The properties of the resonant losses observed in the afterglow plasmas in the rational cases of the  $l=2$  stellarator field are investigated and the shear effect on the resonant losses is examined by superposing the  $l=3$  helical field. It is found that the plasma loss is due to the onset of dissipative drift instability including toroidal effects. The observed properties of the fluctuations such as the frequency, the wave propagation etc. can be explained by the instability. The introduction of

---

Permanent address:

\* Central Research Laboratory, Hitachi Limited, Kokubunji,  
Tokyo, Japan.

\*\* Department of Physics, Tokyo University of Education,  
Tokyo, Japan.

weak shear (shear length  $L_s \sim 300$  cm) reduces the resonant loss in our experimental conditions. When the instability is suppressed, the confinement time becomes long ( $\tau \simeq 60 \sim 200$  ms,  $T_e = 0.6$  eV,  $B_t \simeq 0.8 \sim 3$  kG).

Ohmic heating of plasma is carried out with a programmed vertical field for equilibrium. The density is about  $5 \times 10^{12}$  cm<sup>-3</sup> and the conductivity temperature is about 120 eV. The plasma current is limited by  $(\iota_I + \iota_h) / 2\pi < 0.5$ , where  $\iota_I$  and  $\iota_h$  are the rotational transform angles due to the plasma current and the helical field, when  $\iota_h / 2\pi < 0.5$ . The confinement time is around that of pseudo-classical one.

## §1. Introduction and Experimental Arrangement

Dependences of plasma transport on the properties of magnetic configuration of stellarator field as well as the plasma parameters are studied using JIPP Ib device. This device is a modification of JIPP Ia of an  $\ell=3$  stellarator [1] and is a hybrid stellarator which equips both  $\ell=2$  and  $\ell=3$  helical windings, so that the rotational transform angle  $\iota$  and the shear parameter  $\theta$  are variable independently [3] ( $\iota / 2\pi \lesssim 0.6$ ,  $\theta \equiv (a^2 / 2\pi R) d\iota / dr = 0 \sim 0.1$ ). The maximum toroidal field is 4 kG and the major radius is  $R=50$  cm. The inner radius of the stainless steel vacuum vessel is 7 cm. The  $\ell=2$  helical winding with the field period  $m=4$  has a minor radius of 12.8 cm with 29 kilo-ampere-turns and  $\ell=3$  helical winding has a minor radius of 9.5 cm with 14.5 kilo-ampere-turns (see Fig.1).

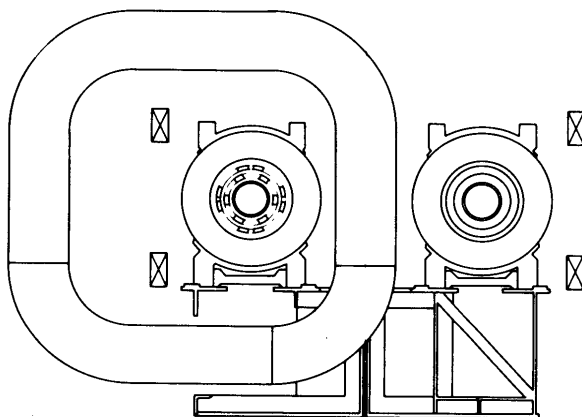


Fig.1. Schematic drawing of JIPP Ib stellarator with  $\ell=2$  and  $\ell=3$  helical windings.

The plasmas are produced by electron cyclotron resonant heating at frequencies of 2.45, 4 and 9 GHz, and by P.I.G. discharge using a small electron emission filament. The base pressure is around  $6 \times 10^{-7}$  torr. The species of filling gases are hydrogen, helium, neon, argon and xenon. The degree of ionization is  $2 \sim 0.2\%$ . The electron density  $n_e$  and the temperature  $T_e$  of the plasma thus produced are  $10^9 \sim 10^{10} \text{ cm}^{-3}$  and  $0.5 \sim 3 \text{ eV}$ , respectively.

The ohmic heating of plasma is carried out using an air core coil with the flux of about 0.02 V-sec and the self-inductance of 1.3 mH. Two capacitor banks of about 25 kJ and 60 kJ are arranged for the time shaping of the induced voltage. An electron source with the applied voltage of 2 kV and the emission current of 0.3 A is used for preionization until 0.2 ms before starting discharge.

As previously reported [1][2], convective cells are observed in afterglow plasma of ECRH, right after switching off the microwave power. These convective motions are damped rapidly with time constant of  $0.4 \sim 0.1 \text{ ms}$  in the case of argon or xenon plasmas due to the ion perpendicular viscosity [2]. After decay of the convective cells, the inward static radial electric field appears and the density fluctuations with the frequency near electron diamagnetic drift frequency appear in the plasma. The fluctuation is due to the  $E_r \times B$  instability [4] which tends to the dissipative drift instability when  $k_{\parallel}$  becomes finite [5]. The inward static radial electric field decreases and the direction of  $E_r$  is reversed. Then the fluctuations fade out and the observed confinement time becomes long in the non-rational case of the rotational transform angle and is about 60 ms when the toroidal field is  $B_t = 0.87 \text{ kG}$ .

## §2. Resonant Loss in Afterglow Plasma and Effect of Shear

When this device is operated as the  $l=2$  stellarator configuration, low frequency fluctuations appear in the afterglow xenon plasma in the rational cases of the rotational transform angle. These fluctuations cause a large diffusion of the plasma and the observed confinement time is one order of magnitude smaller than that of the non-rational case as was observed in the experiments of the references [6] [7]. In Fig. 2a, the confinement of the xenon plasma is shown as a function of the rotational transform angle. The sharp dips are observed in the plotted curve at the rational transform angles.

When the shear is introduced by superposing the  $l=3$  helical field in addition to the  $l=2$  helical field, the observed resonant losses at the rational transform angles are reduced.

Figure 2b and 2c show such experimental results in the conditions that the ratio of the  $l=3$  helical coil current  $I_{h3}$  to the  $l=2$  helical coil current  $I_{h2}$  is kept to be 0.5 and 0.75, respectively, while the rotational transform angle is given by  $t_h/2\pi = 0.013 (I_{h2}/B_t)^2 + 1.14 \times 10^{-3} \cdot r^2 (I_{h3}/B_t)^2$  (r in cm,  $I_h$  in kAT,

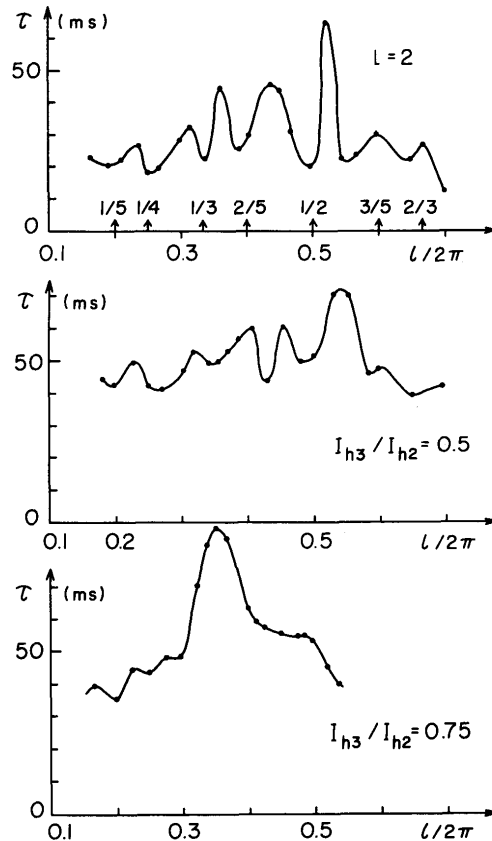


Fig.2. The dependence of the confinement time  $\tau$  of xenon plasma on the rotational transform angle at the outmost magnetic surface, while the ratio of ampere-turns of  $l=3$  to  $l=2$  helical coils is kept to be 0, 0.5 and 0.75, respectively. The toroidal field is  $B=1.4$  kG and the filling pressure of xenon is  $p_0=1.4 \times 10^{-5}$  torr.

$B_t$  in kG). From these figures, one sees that the dip-structure of the curves of confinement time versus the transform angle becomes smooth and the confinement time increases when the shear is introduced. The dependences of the confinement time and the fluctuation level  $\tilde{n}$  on

the shear are shown in Fig.3, where the transform angle is kept to be constant ( $\iota_h/2\pi=0.5$ ) at the plasma boundary. When the shear parameter is made to be larger than  $0.01 \sim 0.015$  at the conditions of  $\iota_h/2\pi=0.5$  and

$B_t=0.87$  kG, the resonant losses and fluctuations are suppressed.

The fluctuations propagate in the direction of the electron diamagnetic drift and they have the poloidal mode number  $m=2$

in the case of  $\iota_h/2\pi=1/2$  and  $m=3$  in the case of  $\iota_h/2\pi=1/3$ , respectively. The toroidal mode number is  $n=1$ . The parallel

component of the propagation vector  $k_{\parallel}=[m(\iota_h/2\pi)-n]/R$  is small near the rational cases. From the observed stabilizing shear parameter ( $\theta \simeq 0.01$ ), we find the critical value of  $k_{\parallel}$  for stabilization by use of the relation  $k_{\parallel}=k_{\perp}(r/2\pi R)(d\iota/dr)\Delta r=(m/2\pi R)(d\iota/dr)\Delta r$ , where  $\Delta r$  is the extent of the region of high level fluctuation. The value of  $k_{\parallel}$  is  $1.5 \sim 2 \times 10^{-3} \text{ cm}^{-1}$  in the case of  $m=2$  and this is approximately equal to the value of  $k_{\parallel}=(m/R)\Delta\iota/2\pi$  estimated from the width  $\Delta\iota$  of the dip in the curve of the confinement time.

The observed frequency, with the correction of the Doppler shift of the rotation due to the radial electric field, is very

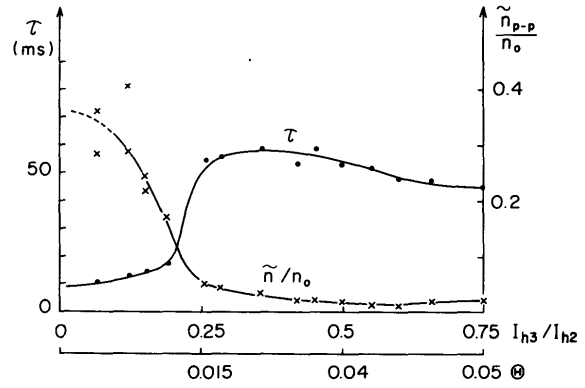


Fig.3. The dependence of the confinement time  $\tau$  and the fluctuation level  $\tilde{n}/n$  near the boundary on the shear parameter  $\theta = a/R (\Delta\iota/2\pi) \simeq (a^2/2\pi R) d\iota/dr$  at the rational case ( $\iota_h/2\pi=0.5$ ) with  $B=0.87$  kG.

low compared with the electron diamagnetic drift frequency  $\omega_{*e}$ . That is,  $\omega_{\text{obs}} - \omega_E \simeq (0.2 \sim 0.3) \times \omega_{*e}$ , where  $\omega_{\text{obs}} \sim 2 \times 10^3$  rad.sec<sup>-1</sup>,  $\omega_E \sim -1 \times 10^3$  rad.sec<sup>-1</sup> (the sense of the  $E_r \times B$  drift is opposite to that of the electron diamagnetic drift) and  $\omega_{*e} \simeq 1 \sim 2 \times 10^4$  rad.sec<sup>-1</sup> in the case of  $m=2$  and  $B_t = 0.87$  kG. The dependence of the observed frequency  $\omega_{\text{obs}}$  on the rotational transform angle is shown in Fig.4a. Figure 4b shows the observed correlation time of ion saturation currents of two probes located at the inner and outer positions in a cross section. The correlation time becomes long only near the rational transform angle.

The phase of density fluctuation  $\tilde{n}$  advances by around 45° to that of the potential fluctuation  $\tilde{\phi}$  (that is  $\tilde{n} \propto \exp(-i\pi/4)\tilde{\phi}$ ) and the particle loss flux  $\langle \tilde{n}(-ik_{\perp}\tilde{\phi})/B_t \rangle$  estimated from the experimental results is consistent with the observed confinement time.

The distributions of the density and the floating potential over a plasma cross section at different times are measured by a movable probe. The density distributions of the xenon plasma in the rational case at  $\iota_h/2\pi=0.5$  and the non-rational case  $\iota_h/2\pi=0.56$  are shown in Figs.5a and 5b, respectively.

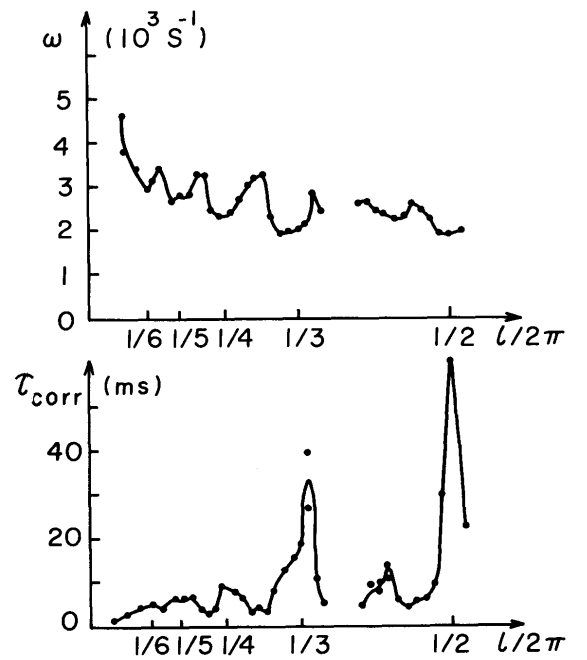


Fig.4. The dependence of the frequency  $\omega$  of the fluctuations on the rotational transform angle. The correlation time  $\tau_{\text{corr}}$  of the ion saturation currents of two probes located at the inner and outer position in the same cross section. The toroidal field is  $B=0.87$  kG.

The effect of collisions with neutrals on the fluctuations is examined by increase of background neutral xenon gas pressure. When the gas pressure is increased, the fluctuations disappear and the resonant losses are suppressed as is shown in Fig.6.

The resonant loss is observed more clearly in cases of the stronger toroidal magnetic field. The width of the resonance becomes narrower and the resonances at larger values of  $2\pi/\iota_h$  appear as is shown in Fig.7. For these

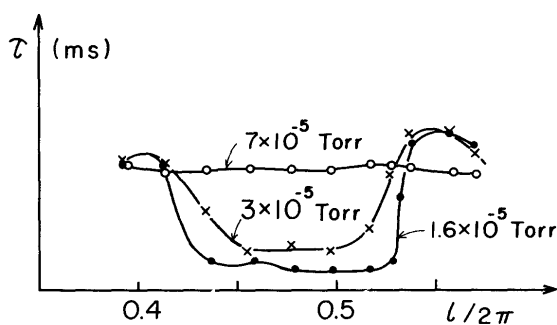


Fig.6. The dependence of the confinement time  $\tau$  on the xenon gas pressure near the rotational transform angle  $\iota_h/2\pi=0.5$ . The parameters are filling gas pressure and the toroidal field is  $B_t = 0.87$  kG.

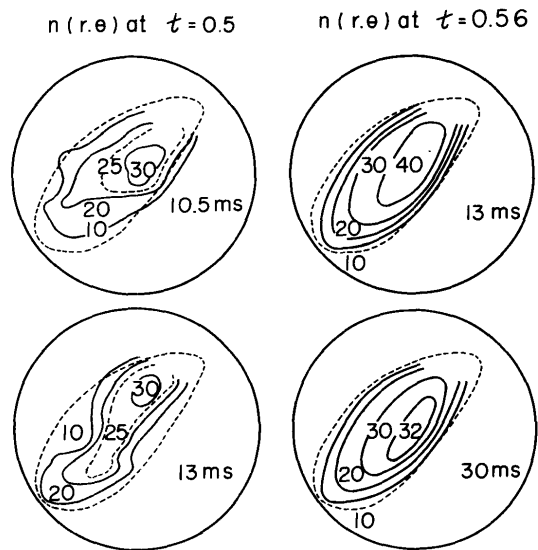


Fig.5. Two dimensional distribution of the density of xenon plasma at the different times in the rational case of  $\iota_h/2\pi=0.5$  (left hand side) and the non-rational case of  $\iota_h/2\pi=0.56$  (right hand side). The numbers in the figures are in arbitrary unit. The toroidal field is 0.87 kG and the radius of wall is 7 cm.

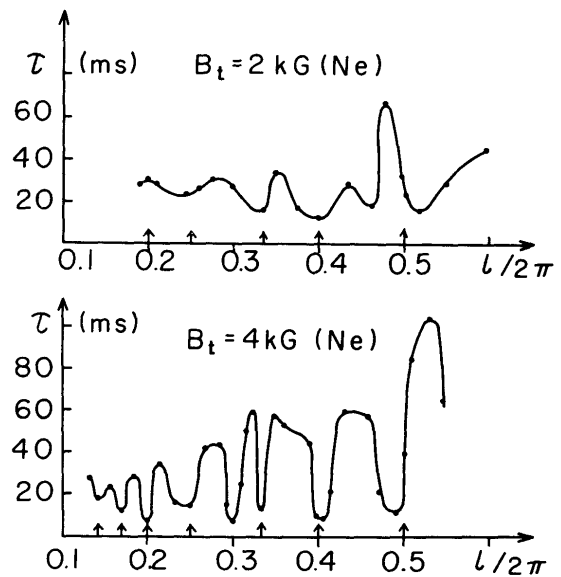


Fig.7. The dependence of the confinement time  $\tau$  of neon plasma on the rotational transform angle in the different magnetic fields.

experiments, the neon plasma produced by the P.I.G. discharge is used.

These experimental results are interpreted in terms of dissipative drift instability including toroidal effects. The dispersion is given by

$$\frac{\omega_{*e} + ik_{\parallel}^2 D_{\parallel}}{\omega + ik_{\parallel}^2 D_{\parallel} - \epsilon \delta \omega_{*e} / \kappa \gamma} = \frac{\omega_{*e} - (T_e / T_i) b (\omega + i\nu_i)}{\omega + b (\omega + i\nu_i)},$$

where  $\kappa^{-1}$  is the scale of the density gradient and  $D_{\parallel} = T_e / m_e \nu_e$ ,  $\epsilon = r/R$ ,  $b = k_{\perp}^2 \rho_i^2$ .  $\nu_i$  is the collision frequency of the ions and neutrals.  $\delta$  denotes the degree of the amplitude variation of the density fluctuation along the poloidal direction and is a quantity less than unity. We find the unstable wave with  $\text{Im}\omega \sim \text{Re}\omega \lesssim 0.3\omega_{*e}$  in the region  $k_{\parallel}^2 D_{\parallel} / \omega_{*e} < 1$  that is  $k_{\parallel} < 10^{-3} \text{ cm}^{-1}$ .

### §3. Experiment of Ohmic Heating with Programmed Vertical Field

Ohmic heating of plasmas confined in the circular stellarator field is carried out with a programmed vertical field. When the vertical field  $B_v = 0$ , the plasma current increases with time and the peak value is limited by  $(\iota_I + \iota_h) / 2\pi < 0.5$ , where  $\iota_I$  and  $\iota_h$  are the rotational transform angles due to the plasma current and the helical field, respectively. In this case, it is observed from the measurements of magnetic probes that the plasma ring shifts outward. The skin time of the stainless-steel vacuum vessel is about 1.8 ms. When the dc vertical field of 20 G is applied, the plasma current rises more slowly and the peak value is smaller than that of the case of  $B_v = 0$ , but the plasma current is maintained without rapid drop.

In order to keep the plasma ring in equilibrium, the vertical field is changed in time with the variation of the plasma current. Fig.8 shows the time variation of the plasma current and the programmed vertical field. In this case the peak value of the current increases to the limit of  $(\iota_I + \iota_h)/2\pi \lesssim 0.5$  and the plasma current is maintained satisfactory.

The average density of the helium plasma measured by an 8 mm microwave interferometer is about  $5 \times 10^{12} \text{ cm}^{-3}$  and the average conductivity electron temperature is  $120 \pm 20 \text{ eV}$  assuming that the effective  $Z$  value is 2. The ion temperature of helium plasma measured by Doppler broadening of HeII line ( $4686 \text{ \AA}$ ) is about 30 eV at around 1.5 msec after the beginning. The estimated energy confinement time of electron is around 0.3 ms which is approximately equal to the pseudo-classical one.

When the rotational transform angle  $\iota_h/2\pi$  of the outmost magnetic surface is smaller than 0.4, the plasma current is limited by the condition  $(\iota_I + \iota_h)/2\pi \lesssim 0.5$  (see Fig.9). When  $\iota_h/2\pi$  is larger than  $0.4 \sim 0.5$ , there is a tendency to follow the condition  $(\iota_I + \iota_h)/2\pi \lesssim 2/3$  or 1.

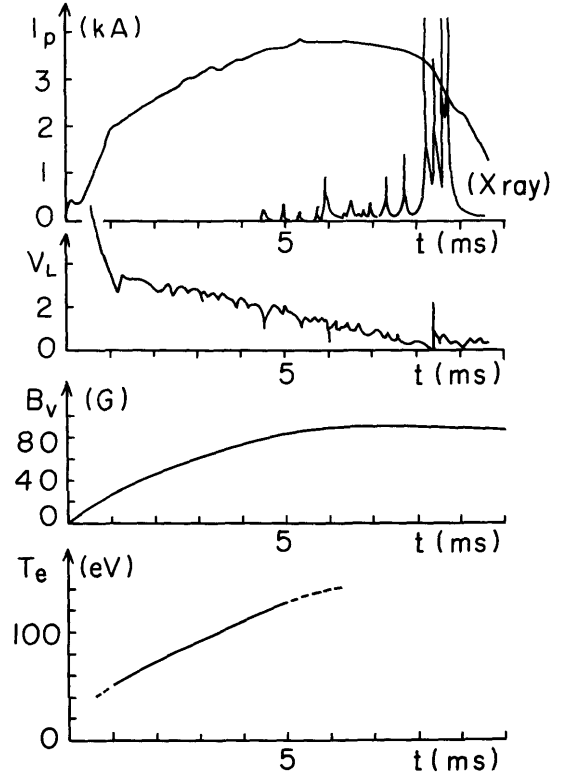


Fig.8. The time variations of the ohmic heating current  $I_p$  (in kA), the loop voltage  $V_L$  (in volt), the observed vertical field  $B_v$  (in G) inside the stainless vacuum vessel and the conductivity electron temperature  $T_e$ . The toroidal field is 4 kG and the rotational transform angle of the  $\ell=2$  stellarator is  $\iota_h/2\pi = 0.1$ . The filling pressure of helium gas is  $10^{-4}$  torr.

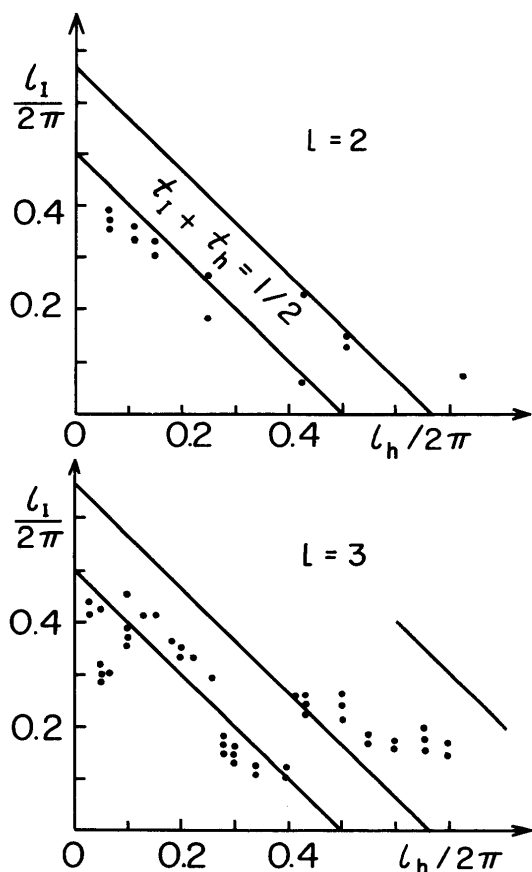


Fig.9. The relation of the rotational transform angles  $l_h/2\pi$  and  $l_I/2\pi$  due to the stellarator field and the plasma current in the case of  $l=2$  stellarator (a) and  $l=3$  stellarator (b). The toroidal field is 2kG and the filling pressure of helium gas is  $10^{-4}$  torr.

#### Acknowledgements

We thank Professor K. Husimi and Professor K. Takayama for their continuous encouragement. We are indebted to Professor R. Itatani and Associate Professor A. Mohri for their useful discussions and to Mr. S. Fujiwaka for his technical assistance.

#### REFERENCES

- [1] K. Miyamoto, A. Mohri, N. Inoue, M. Fujiwara, K. Yatsu, Y. Terashima and R. Itatani; Plasma Phys. and Controlled Nucl. Fusion Res. Madison Conf. Proc. III, p.93 (IAEA, Vienna, 1971)
- [2] M. Fujiwara and K. Miyamoto; Nucl. Fusion 12, 587 (1972)
- [3] K. Miyamoto; Nucl. Fusion 13, 179 (1973), M. Fujiwara, K. Kawahata, A. Mohri and K. Miyamoto; 6th European Conf. on Controlled Fusion and Plasma Phys. p.125 (1973)
- [4] T. Dodo, M. Fujiwara, K. Miyamoto, A. Ogata; 6th European Conf. on Controlled Fusion and Plasma Phys. p.121 (1973), T. Dodo, M. Fujiwara, A. Ogata and K. Miyamoto; to be published in Nucl. Fusion.
- [5] For example, F. F. Chen; Phys. Fluids 8 1323 (1965)
- [6] G. Grieger, W. Ohlendorf, H. D. Pacher, H. Wobig and G. H. Wolf; Plasma Phys. and Controlled Nucl. Fusion Res. Madison Conf. Proc. III, p.37 (IAEA, Vienna, 1971)
- [7] D. K. Akulina, E. D. Andryukhina, Yu. I. Nechaev, O. I. Fedyanin and Yu. V. Kholnov; ibid. III, p.21 (1971)